



Multilevel Monitoring System for Road Networks: Anomaly Detection at the Network and Road-Segment Levels

Hojat Behrooz, S.M.ASCE¹; and Mohammad Ilbeigi, Ph.D., M.ASCE²

Abstract: This study introduces a novel multilevel disruption detection method for road networks. The proposed monitoring and disruption detection method can detect disruptions at both the network and road-segment levels simultaneously. The monitoring process begins with a short-term prediction of hourly traffic speed on each road segment of the network using long short-term memory (LSTM) artificial neural networks. The prediction errors on each road segment at each timestep are used as a proxy to detect disruptions. Network-level disruptions are detected using a multivariate cumulative sum (MCUSUM) control chart. Local disruptions at a road-segment level of granularity are detected by decomposing the monitoring statistic of the MCUSUM control chart that follows a quadratic form using the correlation-maximization (corr-max) transformation. The proposed method was applied to the road network of Manhattan in New York City to examine its performance in detecting disruptions caused by Hurricane Sandy in 2012. The outcomes indicated that the proposed method could detect disruptions precisely at both network and road-segment levels. Whereas existing solutions can either monitor the entire network as a whole or focus on one or a limited number of road segments, the proposed method in this study can recognize if the entire network has been disrupted and also can recognize the road segments that are experiencing unusual traffic patterns. The outcomes of this study set the stage for transportation agencies and decision makers to design adaptive traffic management systems using real-time disruption detection at the network and road-segment levels. **DOI: 10.1061/JTEPBS.TEENG-8391.** © 2024 American Society of Civil Engineers.

Author keywords: Multilevel monitoring; Anomaly detection; Road networks; Long short-term memory (LSTM); Multivariate cumulative sum (MCUSUM); Quadratic decomposition.

Introduction

Transportation networks are the nervous system of an urban environment. The ability to systematically monitor traffic patterns in road networks to detect disruptions and unusual traffic patterns on a real-time basis is a vital component of intelligent transportation systems. Reliable disruption-detection systems enable transportation agencies and decision makers to respond effectively to disruptions and manage transportation systems to avoid cascading failures in the network. Disruption detection systems for road networks also play a vital role in disaster management and during emergency operations such as urgent evacuations. Due to this vital role of road networks in timely, efficient, and successful emergency services, the first Emergency Support Function (i.e., ESF #1) of the FEMA focuses on transportation systems (DOT 2016). The EFS #1 indicates that

the ability to sustain transportation services, mitigate adverse economic impacts, meet societal needs, and move emergency relief personnel and commodities will depend on effective transportation decisions at all levels. Unnecessary reductions or restrictions to transportation will directly impact the

Note. This manuscript was submitted on November 7, 2023; approved on March 1, 2024; published online on May 15, 2024. Discussion period open until October 15, 2024; separate discussions must be submitted for individual papers. This paper is part of the *Journal of Transportation Engineering, Part A: Systems*, © ASCE, ISSN 2473-2907.

effectiveness of all prevention, preparedness, response, recovery, and mitigation efforts. (DOT 2016)

EFS #1 requires transportation agencies and their support departments to monitor and report the status of transportation systems and infrastructures due to an incident. This monitoring process is especially critical during evacuation and recovery operations. Recent natural disasters showed that road transportation networks mainly fail due to unusual traffic patterns before the disaster (e.g., during evacuations) and/or after the disaster (e.g., during recovery). For example, evacuation operations in Texas before Hurricane Rita in 2005 led to a more than 100-mi-long traffic gridlock that took more than 1 day to clear and resulted in a totally failed evacuation plan (Blumenthal 2005). The combination of severe gridlock and excessive heat led to more than 90 deaths even before the storm arrived (Levin 2015). In 2012, when Hurricane Sandy hit New York City (NYC), major disruptions in the NYC road network occurred after the Hurricane when many people returned to the city and recovery operations began (Donovan and Work 2017; Ilbeigi 2019a, b). The substantial need for traffic monitoring systems is not restricted to large-scale humancaused or natural disasters. Any occasional event (e.g., accidents, festivals, and social events) resulting in unusual traffic patterns may lead to unexpected gridlocks and require such a monitoring process.

Existing Methods and Their Limitations

The existing literature on traffic monitoring and disruption detection methods can be categorized into three main groups. The first group of studies used various classification methods, including support vector machines (Xiao 2019; Parsa et al. 2019; Yao et al. 2014), random forests (Su et al. 2022; Dogru and Subasi 2018), and artificial

¹Ph.D. Candidate, Dept. of Civil, Environmental, and Ocean Engineering (CEOE), Stevens Institute of Technology, Hoboken, NJ 07030. Email: hbehrooz@stevens.edu

²Assistant Professor, Dept. of Civil, Environmental, and Ocean Engineering (CEOE), Stevens Institute of Technology, Hoboken, NJ 07030 (corresponding author). ORCID: https://orcid.org/0000-0001-6576-3808. Email: milbeigi@stevens.edu

neural networks (e.g., Li et al. 2016; Zhu et al. 2018; Srinivasan et al. 2008) to categorize and label historical traffic data into normal and abnormal observations. The main limitation of these studies for proactive and real-time disruption detection is their retrospective approach. These methods can differentiate anomalous traffic patterns only in historical data, and have limited power in real-time traffic monitoring and proactive traffic management systems.

The second group of studies developed data-driven methods to detect unusual traffic patterns at the network level. Those studies considered and monitored the entire network as a whole. For example, Donovan and Work (2017) used historical traffic data to develop benchmark probability distributions for the usual travel pace (i.e., travel time divided by distance) in the network and used it to identify unusual traffic patterns. Ilbeigi (2019a) proposed a method to monitor the variations in the network topological features, such as the closeness centrality index, and used it to examine whether the road network is experiencing statistically significant disruptions. Hu et al. (2022) employed a semisupervised autoencoder approach to detect traffic disruptions by monitoring spatiotemporal patterns in origin-destination (OD) mobility data represented as a timedependent directed graph. Although the methods proposed in those studies effectively can detect network-level disruptions, they cannot detect local disruptions and do not offer a solution to detect traffic disruptions at the road-segment level. This limitation is a major obstacle preventing these methods from supporting data-driven traffic management systems effectively during extreme events.

The third group of studies took an entirely different approach than the second group. They focused on individual road segments. The studies in this group proposed methods to monitor traffic patterns in one road segment and detect disruptions based on historical variations in traffic data. The overall approach in these studies was to use nonanomalous historical traffic data in a road segment to provide short-term forecasts of traffic flows and detect traffic states that fall outside the prediction's confidence intervals as disruptions. For example, Tang and Gao (2005) developed a nonparametric regression model to forecast traffic flow on a road and detect abnormal traffic patterns using the standard deviation. Abanto et al. (2013) used autoregressive integrated moving average (ARIMA) time series models and the quantum frequency algorithm (QFA) to conduct short-term traffic forecasting and detect unusual traffic patterns based on the confidence intervals of the predictions. Zhang et al. (2021) used an autoencoder model augmented with spatiotemporal data, including weather conditions to monitor a bus trajectory and detect disruptive situations. Evans (2020) devised a disruption detection algorithm for individual loop detectors using a contextbased random forest model. The proposed solution uses the quantile random tree regression (QRTR) method to determine prediction intervals. If three observations in a row fall outside this interval, the algorithm considers it to be an unusual pattern.

A critical limitation of the methods proposed in this group of studies is their lack of scalability to monitor a large number of road networks simultaneously. Specifically, the performance of these methods considerably drops when they aim to monitor many road segments. This lack of performance is due to computational costs and the methods' approach to considering the road segments individually. In this setting, even if sufficient computational power were available to monitor thousands of roads concurrently, a large number of false alarms would appear at any significance level (Chen 2010) (typically 5%).

Objective

© ASCE

An effective road traffic monitoring network must be able to monitor the entire network and its road segments together in order to

provide valuable and timely information for traffic management systems under the stress of extreme events such as natural disasters. As the review of the existing literature shows, the current traffic monitoring solutions are not able to monitor the road network and all its road segments simultaneously. Motivated by this critical limitation, the overarching objective of this study was to create a novel road traffic monitoring method that can detect disruptions at both network and road-segment levels in one step.

The proposed disruption detection mechanism in this study uses deep learning solutions to forecast hourly travel speed at each road segment in one step. It then uses the prediction errors as inputs for multivariate statistical process control charts to detect network-level disruptions. At the same time, it detects road segment—level disruptions by quantifying the contributions of each road segment in the network disruptions using a decomposition method for quadratic equations.

The remainder of this paper is structured as follows to introduce the proposed method and evaluate its performance. First, we present the proposed method and the required steps to be conducted. Next, we apply the method to the road network of Manhattan in NYC to detect traffic anomalies caused by Hurricane Sandy in 2012 to evaluate its effectiveness. We then summarize the paper's primary contribution to the core body of knowledge and outline potential future research directions in the "Conclusion" section.

Methodology

The proposed multilevel traffic disruption detection method for road networks involves three capabilities: (1) short-term traffic speed prediction, (2) multivariate statistical process control, and (3) contribution assessment through the decomposition of quadratic equations.

First, using historical data on the road network, hourly traffic speed on each road segment is predicted using long short-term memory (LSTM) artificial neural networks. The prediction model conducts a one-point-ahead prediction using a sliding time window with a fixed size of 24 h. The proposed LSTM prediction model is able to forecast the hourly traffic speed on all road segments concurrently. This capability offers three essential advantages. First, the computational cost is considerably lower than the cost of individual predictions for each road. Second, the entire prediction process is faster, making it possible to conduct real-time analysis. Third, the prediction model incorporates spatiotemporal interdependencies among the traffic patterns in the road segments in the forecasting process instead of considering them independent from each other. This considerably improves the accuracy of the model and its prediction power.

Although the LSTM prediction model is able to accurately forecast the hourly traffic speed on each road, similar to any other model, its prediction is not perfect, and the predicted values are subject to error. The prediction errors can be used as a proxy to monitor traffic disruption. Specifically, because the LSTM prediction model is trained using usual traffic patterns and data, we hypothesize that if a disruption occurs, the prediction power of the model will decrease significantly, and there will be a considerable increase in the error values. Monitoring prediction errors as a proxy to control a process is a well-established approach and has been used in many previous studies in various domains, such as multivariate control performance assessment (Zhao et al. 2010), electrical motors' predictive current control (Siami et al. 2016), and control design and fault diagnosis (Campestrini et al. 2017).

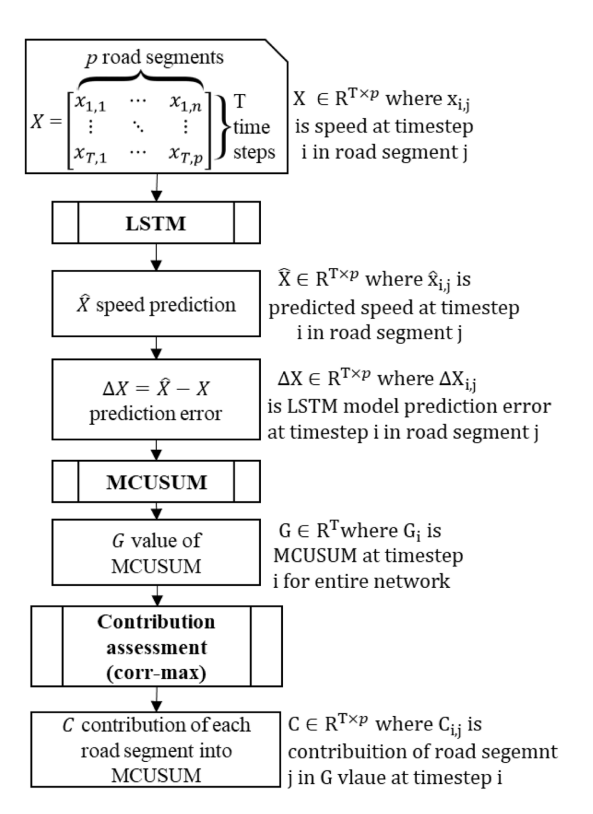


Fig. 1. Steps conducted in the proposed multilevel disruption detection mechanism for road networks.

To detect disruptions at the network level, the prediction errors in each road segment are monitored collectively using a multivariate cumulative sum (MCUSUM) control chart. The input data for the control chart is a vector. Each vector dimension represents the prediction error for hourly travel speed on each road segment at a specific time. Therefore, the data set can be represented by a $p \times T$ matrix, where p is the number of roads, and T is the number of observations through time on that road segment. As suggested by Pignatiello and Runger (1990), the MCUSUM control chart uses the Mahalanobis distance measure (Mahalanobis 1936) to combine different dimensions of the input vector and monitor the road network as a whole.

Whereas the MCUSUM control chart monitors the network as a whole and detects network-level disruptions, at each point in time the roads that have anomalous traffic patterns can be detected based on their contribution to the MCUSUM's calculated monitoring statistic. Specifically, the MCUSUM control statistic has a quadratic form (Pignatiello and Runger 1990), and the contribution of each road segment to the value of that statistic at each point in time is assessed using a method proposed by Garthwaite and Koch (2016).

Fig. 1 summarizes the proposed method to develop a multilevel disruption detection mechanism for road networks. The following sections briefly review the overall structure of the LSTM prediction model, the MCUSUM control chart, and the contribution assessment method. More detailed information is provided in the "Implementation and Assessment" section, in which we apply the proposed method to the road network of Manhattan in NYC.

Short-Term Prediction Using LSTM Networks

The original version of LSTM networks was introduced by Hochreiter and Schmidhuber (1997). However, throughout the years, many researchers refined and improved the method. LSTM

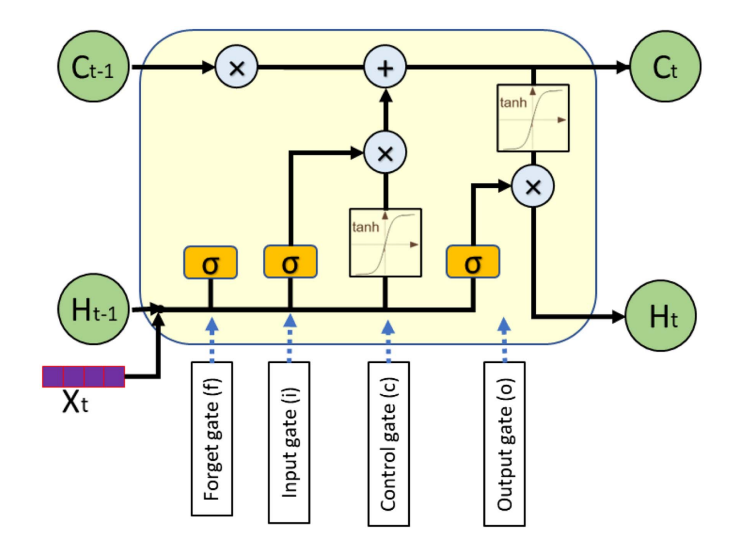


Fig. 2. Overall structure of the LSTM networks.

networks are a special form of recurrent neural networks (RNNs) that are able to consider and analyze a long-term chain of information without suffering from the vanishing and exploding gradients problem (Basodi et al. 2020). Specifically, LSTM networks can effectively recognize the optimal amount of information in sequential data and selectively memorize or forget information over extended periods to adjust the decay of statistical dependency dynamically and produce more-accurate predictions. The selective memorization capability also facilitates capturing nonlinear relationships in complex systems, big data analysis, and robustness to noise and missing data (Goodfellow et al. 2016).

The cornerstone of the LSTM structure is the cell state that retains information over time and enables capturing long short-term dependencies. LSTM networks contain a series of connected cells to create a recurrent network. Each cell's output serves as the next cell's input, enabling the propagation of information throughout the network. Information in a cell state is managed using a gate mechanism. Typically, LSTMs are equipped with four types of gates: (1) forget gates (f), (2) input gates (i), (3) control gates (c), and (4) output gates (o). Fig. 2 shows the overall structure of the LSTM networks; C_t is the cell state at time t, H_t is the unit output at time t, H_t is the input signal at time H_t or represents an activation function operation, denotes an element-wise multiplication of vectors, and H_t indicates vector summation.

The mathematical expressions for gate functions and cell state features are as follows:

$$f_t = \sigma(W_{xf}X_t + W_{hf}h_{t-1} + b_f) \tag{1}$$

$$i_t = \sigma(W_{xi}X_t + W_{hi}h_{t-1} + b_i)$$
 (2)

$$o_t = \sigma(W_{xo}X_t + W_{ho}h_{t-1} + b_o)$$
 (3)

$$c_t = \sigma(W_{xc}X_t + W_{hc}h_{t-1} + b_c) \tag{4}$$

$$c_t = (f_t \times c_{t-1} + i_t \times \tanh(W_{xc}X_t + W_{hc}h_{t-1} + b_c))$$
 (5)

$$h_t = o_t \times \tanh(c_t) \tag{6}$$

where W_{xf} , W_{xi} , W_{xo} , W_{xc} , W_{hf} , W_{hi} , W_{ho} , and W_{hc} are the corresponding weight matrices; and b_f , b_i , b_o , and b_c are the corresponding bias vectors. The bias vector gives the ability to adjust values to prioritize or deprioritize information, regulate memory

retention, and impact output generation based on input sequence context. It introduces adaptability and fine-tuning to the LSTM's memory cell, enhancing the network's capability to capture longterm dependencies in sequential data.

Each element of the input data (i.e., traffic speed on a road segment at a specific time) is featured using a series of weighted binary neurons (typically 32 or 64 units). These neuron units communicate the information among the cell states. The LSTM model is adaptable to any form of transportation network and can be implemented in any urban setting, because it can adjust its features actively and dynamically to discover spatiotemporal traffic patterns during the training process. This capability is facilitated by iteratively updating the associated weights to each connection between two neurons in the recurrent neural network, representing traffic temporal interconnectivity between two roads. The ability to adjust the weights dynamically allows the model to capture varying traffic conditions and improves the prediction power and fitness of the model while maintaining its flexibility and adaptability to any form of road network and traffic patterns. In each iteration of the training process, the weights are adjusted using a back-propagation algorithm to minimize the error between the predicted and actual values (Sherstinsky 2020). Specifically, for a given weight w_{ij} connecting neuron i to neuron j, the weight adjustment (Δw_{ij}) can be expressed using a gradient descent formulation

$$\Delta w_{ij} = -\eta \frac{\partial L}{\partial w_{ij}} \tag{7}$$

where Δw_{ij} = change in weight; η = learning rate, which controls the step size of the update; and $\partial L/\partial w_{ij}$ is the partial derivative of the loss function L with respect to the weight w_{ii} .

Solving the partial derivative determines weight adjustments to minimize the error between the predicted and actual values. As the model learns from historical data in each iteration, it dynamically quantifies the temporal impact of each road segment on the traffic of other roads by updating the weights of the corresponding interconnected neurons. Further detailed information about LSTM networks was presented by Goodfellow et al. (2016).

The final output of the LSTM prediction is a time series of travel speed at each point of time on each road segment. The predicted values are compared with the actual observations, and a time series of prediction errors is created for each road segment. A p (i.e., number of road segments) $\times T$ (i.e., length of time series) matrix consisting of the prediction error times series is the input for the network monitoring mechanism using the MCUSUM control chart.

Network Monitoring Using MCUSUM

© ASCE

Statistical process control methods offer systematic approaches to monitor variations in a variable over time, characterize its usual patterns, and define thresholds to detect any statistically significant change (if any). One of the powerful and sensitive statistical process control methods is the CUSUM control chart. CUSUM control charts have been used in various areas, such as quality control in manufacturing (Wu et al. 2009), market analysis (Ilbeigi et al. 2017), and infrastructure resilience (Ilbeigi and Dilkina 2018). A CUSUM control chart monitors a time series by accumulating deviations of each observation from the mean of the series.

When the input data is a vector, an extended version of the CUSUM, the multivariate cumulative sum (MCUSUM), control chart must be used. A MCUSUM control chart monitors the joint behavior of multiple dimensions of the vector collectively. There are various versions of the MCUSUM control chart that use different approaches to model the collective behavior of different dimensions in the input vector. In this study, we used the method

proposed by Pignatiello and Runger (1990) due to its sensitivity to small shifts. This approach is based on the Mahalanobis distance measure (Mahalanobis 1936) and defines the monitoring statistic, G_i , as follows:

$$G_i = \max\left[\sqrt{C_i^T \Sigma_0^{-1} C_i} - 0.5(\mu_1 - \mu_0)^T \Sigma_0^{-1} (\mu_1 - \mu_0) n_i, 0\right]$$
(8)

where G_i is the monitoring statistic that captures the cumulative deviations of the observations, and is equal to zero at the beginning (i.e., $G_0 = 0$); μ_0 is a $p \times 1$ vector that represents the average traffic speed prediction error in each road segment of the network during in-control periods, where p = road segments in network; μ_1 is a $p \times$ 1 vector that represents the threshold for out-of-control scenarios; Σ_0 is a $p \times p$ matrix that denotes the variance-covariance of the incontrol traffic speed prediction error in the road segments; n_i is a counting factor calculated as follows:

$$n_{i} = \begin{cases} n_{i-1} + 1, & \text{if } G_{i-1} > 0\\ 1, & \text{otherwise} \end{cases}$$
 (9)

and C_i is a $p \times 1$ vector that shows the deviation of the *i*th observation from the in-control mean vector, μ_0

$$C_i = \sum_{l=i-n_i+1}^{i} (X_i - \mu_0)$$
 (10)

where X_i is a $p \times 1$ vector that represents traffic speed prediction error on each road segment at time i.

The MCUSUM control chart constantly calculates and monitors G_i against a control limit. The control limit, H_i is determined based on the in-control average run length (ARL₀) (Montgomery 2020). The ARL₀ value is the expected number of observations until the control chart signals for an out-of-control observation, if the entire process is still in control, meaning that the detected out-of-control observation is a random event without a persistent shift pattern. When the ARL₀ is longer than the length of the available in-control historical observations, more in-control observations are generated using simulations based on the Markov chain Monte Carlo method (Brook and Evans 1972; Gamerman and Lopes 2006).

In a MCUSUM control chart, G_i is a scaler that captures the collective variations of all dimensions in the input vector and has a quadratic form. Therefore, the original MCUSUM control chart can only monitor the entire network as a whole, and cannot detect unusual traffic patterns at the road-segment level of granularity. To address this limitation, we propose a method to augment the MCUSUM control chart with a decomposition procedure for quadratic equations inspired by the corr-max transformation method introduced by Garthwaite and Koch (2016). This method can quantify how different road segments contribute to the calculated G_i value at each point in time. The method is reviewed in the next section.

Road Segment Monitoring Using Contribution Assessment Method

The main idea of the proposed method to detect disruptions at the road-segment level involves the fact that the MCUSUM monitoring statistic, G_i , has a quadratic form. Garthwaite and Koch (2016) proposed a decomposition method for quadratic equations as follows:

$$W^{T}W = (X - \mu_{0})^{T} \Sigma_{0}^{-1} (X - \mu_{0})$$
(11)

J. Transp. Eng., Part A: Systems

where W is a $p \times 1$ vector.

The identity matrix of W (i.e., the product of W and its transpose) gives G_i . Therefore, each element of W represents the contribution of that dimension to the calculated value of G_i . For example, if the jth element of W is close to zero, the jth dimension of the X_i (i.e., the error of traffic speed prediction on the jth road segment at time i) does not have a considerable contribution to the magnitude of G_i . Therefore, it can be concluded that the traffic on that road segment has not been disrupted significantly. Conversely, if the absolute value of the kth element of W is considerably larger than zero, the traffic on the kth road segment at time i has been disrupted, with a considerable contribution to the calculated G_i .

The remaining challenge is to determine W and its elements. Garthwaite and Koch (2016) proposed a method, called corr-max transformation, to determine W. The corr-max method proposes a transformation function that maximizes the sum of correlations between individual variables and their transformed counterparts.

Implementation and Assessment

Data Set Description

To empirically examine the effectiveness of the proposed disruption detection method, we applied it to the road network of Manhattan in NYC and assessed its performance in detecting traffic disruptions due to Hurricane Sandy in 2012. Hurricane Sandy was one of the most disruptive natural events in the history of the United States (Klotzbach et al. 2022). The storm formed on October 22, 2012, and impacted the NYC area on October 29, 2012. The NYC traffic data are a publicly available data set prepared by Donovan and Work (2017). This data set contains hourly average travel time on each road segment of the NYC road network estimated using historical trajectories of nearly 700 million taxi trips in NYC from January 2010 to December 2013. It also includes the coordinates and length of each road segment. Using this information, the hourly average travel speed in each road segment can be calculated. The data set contains 8,839 road segments, represented by 3,910 nodes and 8,839 links.

Data Preprocessing

The LSTM model was trained using traffic data from January 1, 2011, to October 10, 2012. The data preprocessing procedure in this study consisted of four main steps. First, we checked the data set for errors or misrecorded data (e.g., a negative travel time). The data set did not have any issues in that regard. Second, because the LSTM model should be trained using usual traffic data, we removed observations during periods in which the NYC road network experienced abnormal disruptions. Donovan and Work (2017) identified disruptions in the NYC road network (at the network level) due to various stressors such as blizzards, storms, and New Year events using this data set. Removing traffic data during the disruption periods led to the elimination of observations at 264 time points.

Considering the nature of the LSTM models, the input data for each road segment need to be a continuous time series without any missing data. However, traffic data sets typically are sparse and have missing observations because many road segments, especially minor ones, may not carry traffic flows recorded through taxi trajectories at all timesteps. Therefore, in this study, we used traffic data from main road segments that did not have more than two consecutive missing values. This set of roads consisted of 1,229 road segments. These road segments covered the majority of the main road segments in Manhattan (Fig. 3). We imputed the missing values using a two-step interpolation technique (Fan et al. 2020). We also tested the data set for interpolating more than two consecutive missing values; however, the result showed that this would lead to



Fig. 3. Road segments for LSTM model training after two-step interpolation. (© OpenStreetMap contributors.)

overfitting and adversely affect the prediction power of the model. Finally, the hourly average traffic speed in the data set was normalized using a minimum-maximum scaler approach to ensure compliance with the LSTM requirements.

LSTM Model Development

To train the model, the input stream of data was arranged into a series of equal-sized subsequences using a sliding time window with a fixed size. Considering the daily cyclical patterns in the traffic data, we considered a sliding window length of 24 h. Therefore, the model uses 24 hourly observations to predict the traffic speed in the following hour and moves the sliding window in 1-h increments.

As suggested by many previous studies on LSTM modeling, such as Brownlee (2017), our short-term prediction model consists of two LSTM layers to improve prediction accuracy. In each layer, 64 units of neurons transform the input matrix into weighted binary data. The model uses a rectified linear unit (ReLU) activation function (Nair and Hinton 2010). This activation function is one of the LSTM features that overcome the vanishing gradient problem by allowing the model to learn faster. The ReLU is a piecewise linear function that outputs the input directly if it is positive; otherwise, it outputs zero. More-detailed information about ReLU activation function was presented by Nair and Hinton (2010).

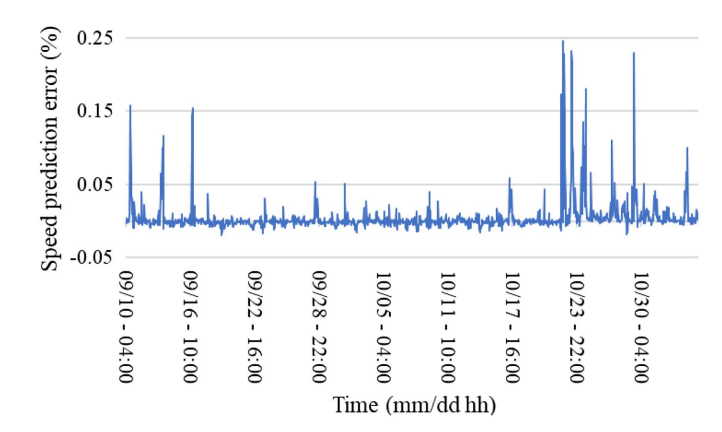


Fig. 4. Sample road segment speed prediction error.

Because traffic data may contain noisy and outlier observations, a dropout method was used in the training process. Dropout is a regularization technique commonly used in neural networks to prevent overfitting and to improve the robustness of the model against noisy data (Srivastava et al. 2014). The dropout strategy involves randomly deactivating (i.e., setting to zero) a percentage of neurons (typically 40%) in the neural network during each training iteration. This introduces an element of randomness to the learning process, forcing the model to learn more-general features and patterns to reduce its reliance on specific data points, especially those that might be noisy or outliers. This regularization technique improves the model's performance on new, unseen data.

The optimization criteria were defined based on the mean squared error (MSE) of predictions using the Adam optimizer (Kingma and Ba 2014). For early stopping conditions, we set the model to abort the training process if the accuracy of the predictions did not improve for five consecutive rounds.

To properly assess the goodness-of-fit and prediction power of the LSTM model, we used 80% of the observations for model

training and 20% for prediction evaluation. The model training process converged in less than 4 min using a workstation equipped with a 12th-generation Intel Core i9 processor and 64 GB memory. The outcomes indicated that the in-sample goodness-of-fit was 99.56%. We then used the remaining 20% of the data to evaluate the prediction power of the model. The results indicated that the out-of-sample prediction accuracy was 99.39%.

Short-Term Prediction Using the LSTM Model

The created LSTM model was used to predict hourly travel speed on each road segment from October 11, 2012, to November 10, 2012, through a one-step-ahead prediction using a 24-h sliding window. Next, the time series of prediction errors for each road segment was calculated. For example, Fig. 4 shows the time series of prediction errors for one of the road segments. These time series re used to create a stream of a vector, X_t , which shows the prediction error in each road segment at time t. The stream of these vectors is the input to the MCUSUSM control chart.

Network-Level Disruption Detection Using MCUSUM Control Chart

Fig. 5 shows the MCUSUM control chart for prediction errors in the network. The control limit, H, was determined to maintain an ARL₀ equal to 10,000, indicating that on average, one false positive alarm may occur every 10,000 consecutive hours. The calculated values for G_i in the control chart indicate that the overall variations in the hourly speed of the traffic network shifted from its natural range on October 29, 2012, at about 11:00 a.m. local time, 10 h before the Hurricane struck NYC. To detect the return point, at which the traffic flow returned to its natural behavior, we conducted a reverse control chart (Ilbeigi and Dilkina 2018). The reverse control chart indicated that the overall variations in the NYC road network returned to their natural behavior on November 2, 2012, at about 11:00 p.m. local time. Therefore, in total, the NYC road network was disrupted for 108 h. These results are aligned with the

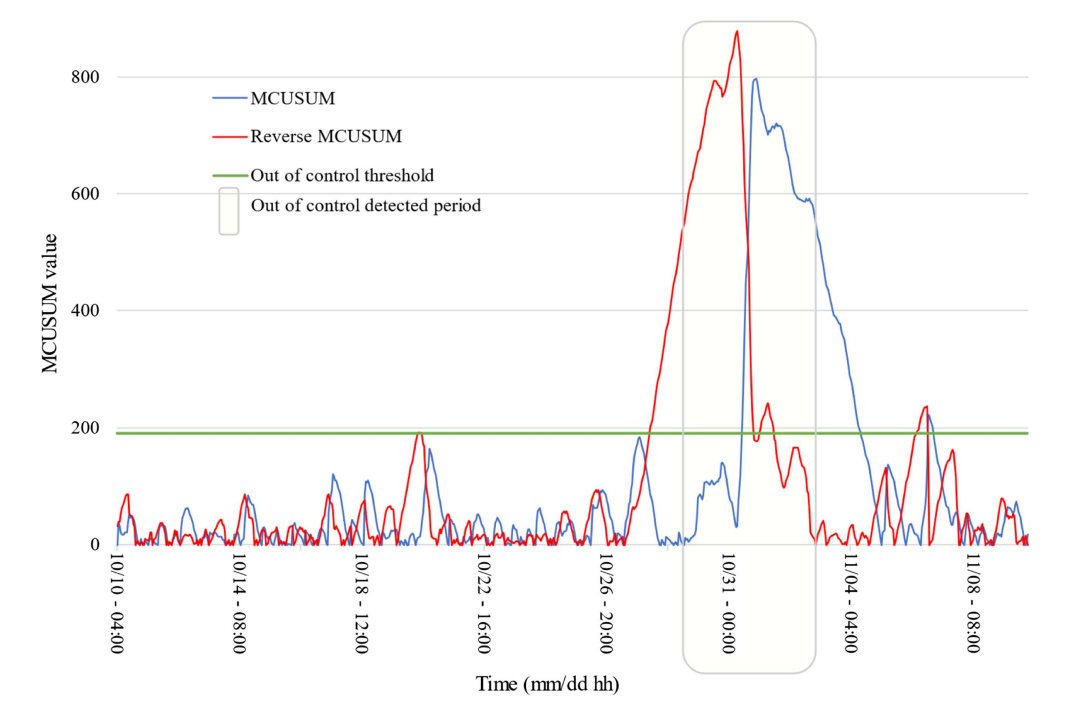


Fig. 5. MCUSUM and the reverse MCUSUM control charts for the network-level disruption detection.

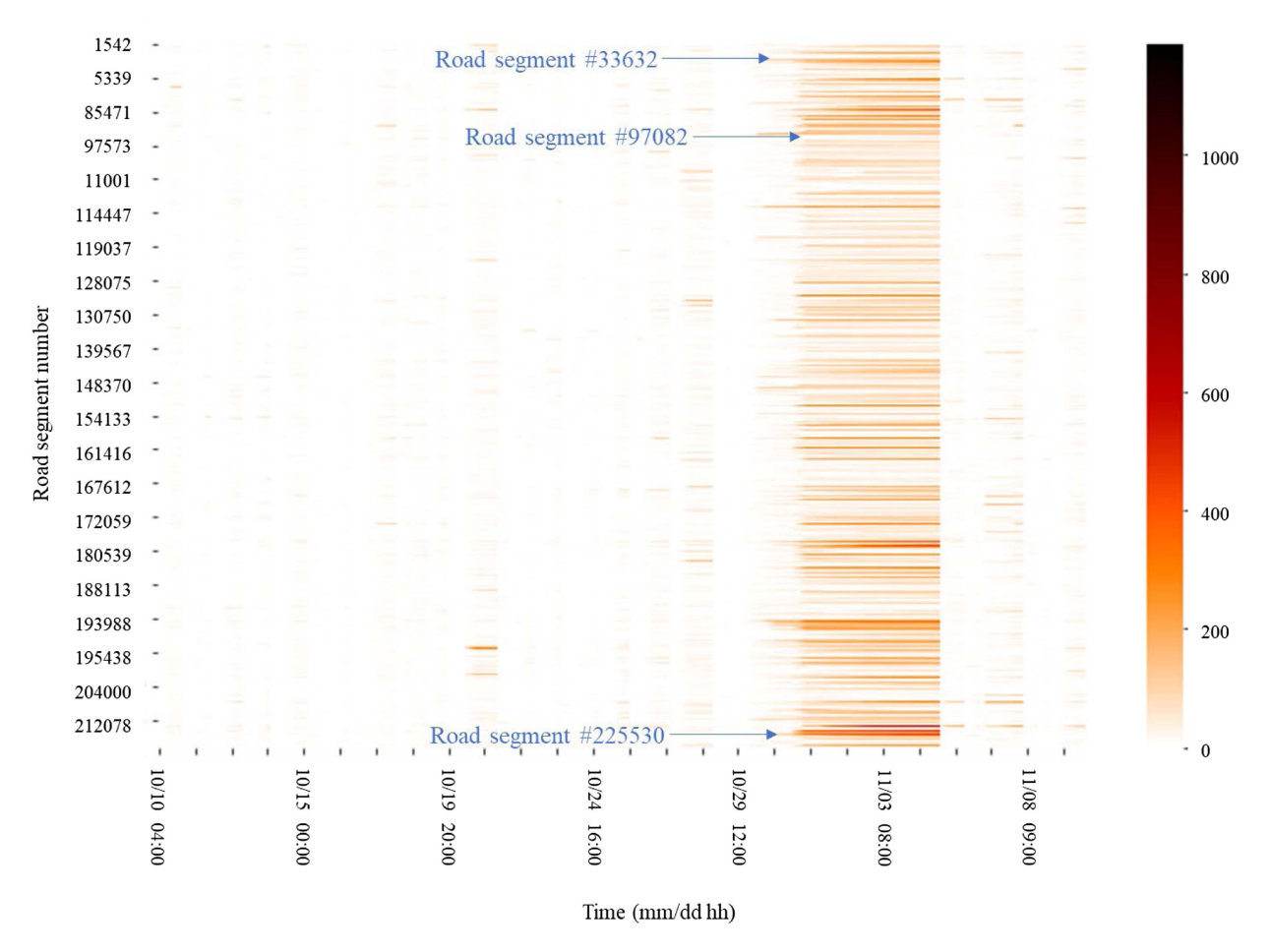


Fig. 6. Road segment-level disruptions using the quadratic contribution assessment.

outcomes of previous studies that evaluated disruptions at a network level, including Donovan and Work (2017) and Ilbeigi (2019a).

Road Segment–Level Disruption Detection Using Contribution Assessment

Road segment disruptions are detected using the contribution assessment method. Fig. 6 displays the contribution of each road segment to the calculated G_i value throughout time. The heatmap clearly shows that a considerable number of roads contributed to the shifted MCUSUM control statistic, G_i , that crossed the control limit during the Hurricane. However, the length and magnitude of their contributions vary. To further investigate the outcomes of the contribution assessment, we focus on a few road segment examples here.

Fig. 7 shows hourly traffic speed on three road segments. The first road segment [Fig. 7(a)] is Road segment 97,082 in the data set, which represents a relatively short segment of 3rd Avenue in residential areas of the Upper East Side. The heatmap in Fig. 6 indicated that this road segment did not make a considerable contribution to G_i . Consistent with this observation, the hourly speed time series of that road segment [Fig. 7(a)] also does not show a significant shift in its variations during the hurricane period, indicating that the Hurricane did not disrupt its traffic pattern. Conversely, the heatmap in Fig. 6 shows that Road segments 225,530 (a road segment of 10th Avenue close to commercial areas at the entrance of Columbus Circle) and 33,632 (a road segment of 8th

Avenue close to the entrance of the Lincoln Tunnel, which is one of the main connectors of Manhattan to New Jersey and was closed during the Hurricane) considerably contributed to the overall disruption of the network. Their hourly speed time series [Figs. 7(b and c)] also confirmed that their traffic patterns significantly changed during the hurricane period. The disruptions in these two road segments were not very similar in terms of the size and duration of the disruptions. The comparison of these three road segments clearly shows the value of a road segment–level disruption detection method that helps decision makers better understand how the network and its elements are under the stress of an extreme event at each point in time.

Conclusions and Future Studies

This study introduces a novel traffic disruption detection method that involves three capabilities: (1) short-term traffic speed prediction using a LSTM model, (2) detecting network level disruptions by monitoring prediction errors using a MCUSUM control chart, and (3) detecting disrupted road segments using a contribution assessment method for quadratic equations based on corr-max transformation. The proposed method was implemented using the Manhattan road network in NYC to examine its performance in detecting disruptions caused by Hurricane Sandy in 2012. The outcomes indicated that the proposed method could effectively and accurately detect disruptions at the network level and also local disruptions at the road-segment level.

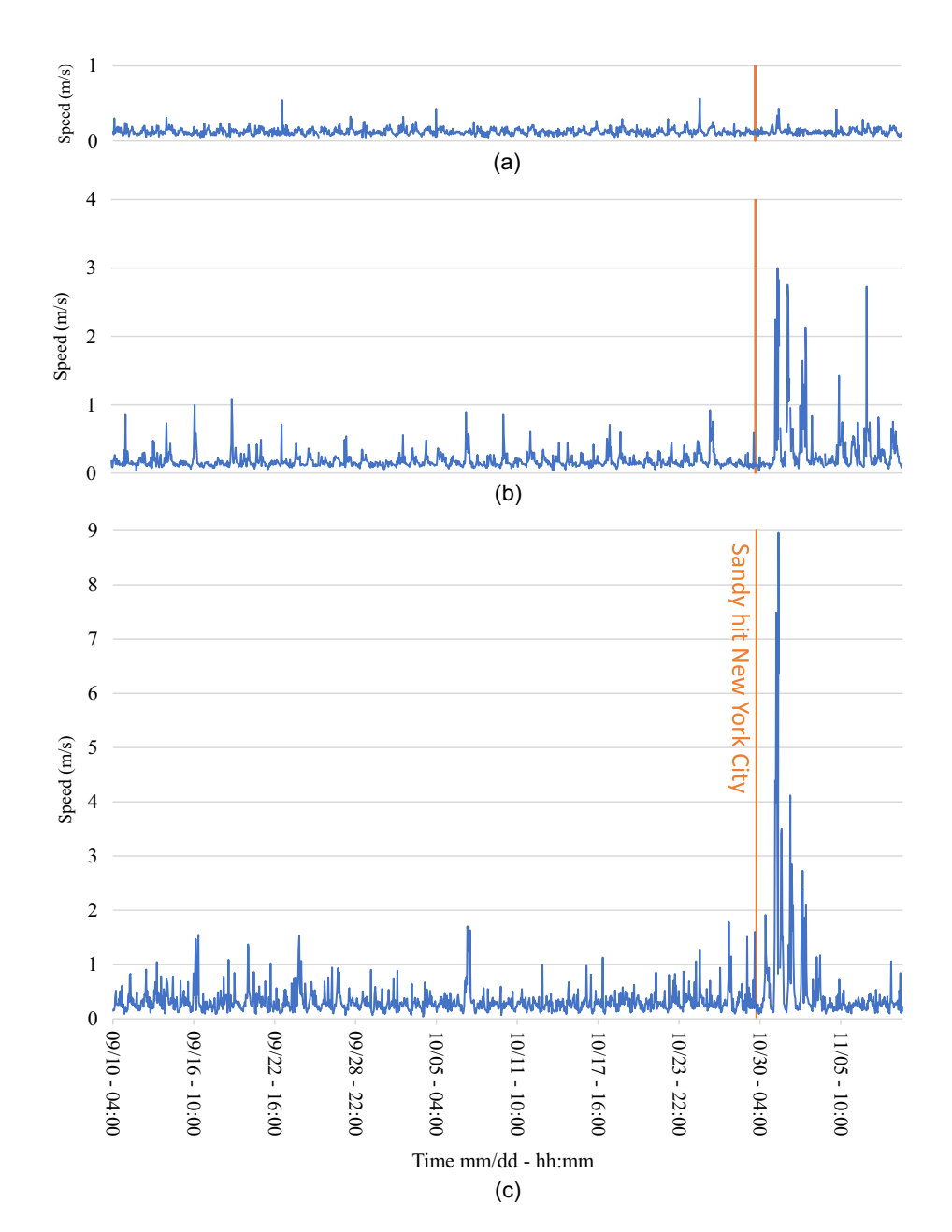


Fig. 7. Hourly traffic speed on three sample road segments with different levels of disruptions during Hurricane Sandy: (a) Road segment 97,082, which was not disrupted; (b) Road segment 225,530, which was disrupted; and (c) Road segment 33,632, which was significantly disrupted.

The primary contribution of this study to the core body of knowledge is the development of a multilevel disruption detection method that can monitor and detect disruptions at both network and road-segment levels simultaneously. In other words, whereas the existing solutions presented in previous studies either can monitor the entire network as a whole or can focus on one or a limited number of road segments, the proposed method in this study can recognize if the entire network has been disrupted and also can determine the road segments that are experiencing unusual traffic patterns. The proposed method is adaptable to various transportation networks with different characteristics and traffic patterns. It can detect anomalous patterns in different situations, including planned events (e.g., a parade) or unexpected and spontaneous events (e.g., natural disasters), regardless of their causes.

This study sets the foundation for developing adaptive and proactive intelligent transportation systems that can recognize local and network-level disruptions on a real-time basis and take corrective actions to alleviate the disruptions. The proposed method can contribute to adaptive intelligent transportation systems for smart traffic metering, especially in the future of road networks when connected autonomous vehicles (CAVs) will have high penetration in the transportation systems. These systems also can play a vital role in emergency management operations in response to extreme events.

Although the implementation and assessment of the proposed method showed promising results, the method is subject to some inherent limitations. One of the major limitations is linked to the LSTM forecasting model. As noted previously, the LSTM model needs a complete time series of hourly traffic data without any missing observations. In reality, traffic data sets are sparse, and there may not be sufficient observations from all roads at all times. This is especially the case for minor road segments that do not carry a considerable traffic volume. As discussed in detail in the previous sections, for the implementation of the proposed method, we addressed this challenge by focusing only on main road segments.

Although this strategy helped us implement and evaluate the proposed method in this study, developing forecasting and monitoring methods with lower sensitivity to missing values or augmenting the method proposed in this study with data imputation solutions such as the one proposed by Nouri et al. (2022) can be a basis for future studies. Furthermore, designing and developing algorithms for adaptive road networks that can react automatically to the detected disruptions to optimize the overall traffic flow in the network can be a target for future studies. Finally, further investigation of the causes of the detected disruptions is another potential topic for future studies.

Data Availability Statement

Some or all data, models, or code that support the findings of this study are available from the corresponding author upon reasonable request.

Acknowledgments

The research presented in this paper was supported by the National Science Foundation under Grant CMMI-2026795. Any opinions, findings, conclusions, or recommendations expressed in this material are those of the authors and do not necessarily reflect the views of the National Science Foundation.

References

- Abanto, J. E., C. C. Reyes, J. A. Malinao, and H. N. Adorna. 2013. "Traffic incident detection and modelling using quantum frequency algorithm and autoregressive integrated moving average models." In *Proc.*, *IISA 2013*, 1–6. New York: IEEE. https://doi.org/10.1109/IISA.2013 6623679
- Basodi, S., C. Ji, H. Zhang, and Y. Pan. 2020. "Gradient amplification: An efficient way to train deep neural networks." *Big Data Min. Anal.* 3 (3): 196–207. https://doi.org/10.26599/BDMA.2020.9020004.
- Blumenthal, R. 2005. "Miles of traffic as Texans heed order to leave." N.Y. Times, September 23, 2005.
- Brook, D., and D. A. Evans. 1972. "An approach to the probability distribution of cusum run length." *Biometrika* 59 (3): 539–549. https://doi.org/10.1093/biomet/59.3.539.
- Brownlee, J. 2017. Long short-term memory networks with python: Develop sequence prediction models with deep learning. Melbourne, VIC, Australia: Machine Learning Mastery.
- Campestrini, L., D. Eckhard, A. S. Bazanella, and M. Gevers. 2017. "Data-driven model reference control design by prediction error identification." *J. Franklin Inst.* 354 (6): 2628–2647. https://doi.org/10.1016/j.jfranklin.2016.08.006.
- Chen, T. 2010. "On reducing false alarms in multivariate statistical process control." *Chem. Eng. Res. Des.* 88 (4): 430–436. https://doi.org/10.1016/j.cherd.2009.09.003.
- Dogru, N., and A. Subasi. 2018. "Traffic accident detection using random forest classifier." In *Proc.*, 2018 15th Learning and Technology Conf. (L&T), 40–45. New York: IEEE.
- Donovan, B., and D. B. Work. 2017. "Empirically quantifying city-scale transportation system resilience to extreme events." *Transp. Res. Part C: Emerging Technol.* 79 (Jun): 333–346. https://doi.org/10.1016/j.trc 2017.03.002
- DOT. 2016. "Emergency Support Function #1—Transportation Annex." Federal Emergency Management Agency. Accessed August 15, 2023. https://www.fema.gov/sites/default/files/2020-07/fema_ESF_1 _Transportation.pdf.
- Evans, J. R. A. V. 2020. "Improving road incident detection algorithm performance with contextual data." Doctoral Dissertation, Dept. of Civil, Maritime and Environmental Engineering, Univ. of Southampton.

- Fan, Y., H. Yang, S. Maheshwari, and Y. Yang. 2020. Improving transportation information resilience: Error estimation for networked sensor data. Davis, CA: Univ. of California, Davis, National Center for Sustainable Transportation.
- Gamerman, D., and H. F. Lopes. 2006. Markov chain Monte Carlo: Stochastic simulation for bayesian inference. Boca Raton, FL: CRC Press.
- Garthwaite, P. H., and I. Koch. 2016. "Evaluating the contributions of individual variables to a quadratic form." Aust. N.Z. J. Stat. 58 (1): 99–119. https://doi.org/10.1111/anzs.12144.
- Goodfellow, I., Y. Bengio, and A. Courville. 2016. *Deep learning*. Cambridge, MA: MIT Press.
- Hochreiter, S., and J. Schmidhuber. 1997. "Long short-term memory." *Neural Comput.* 9 (8): 1735–1780. https://doi.org/10.1162/neco.1997.9.8 .1735.
- Hu, Y., A. Qu, and D. Work. 2022. "Detecting extreme traffic events via a context augmented graph autoencoder." ACM Trans. Intell. Syst. Technol. (TIST) 13 (6): 1–23. https://doi.org/10.1145/3539735.
- Ilbeigi, M. 2019a. "Statistical process control for analyzing resilience of transportation networks." *Int. J. Disaster Risk Reduct.* 33 (Feb): 155–161. https://doi.org/10.1016/j.ijdrr.2018.10.002.
- Ilbeigi, M. 2019b. "Statistical process control for quantifying resilience of transportation infrastructures using GPS data: Hurricane Sandy case study." In *Proc.*, CIB Annual Conf. Ottawa: International Council for Research and Innovation in Building and Construction.
- Ilbeigi, M., D. Castro-Lacouture, and A. Joukar. 2017. "Generalized autoregressive conditional heteroscedasticity model to quantify and forecast uncertainty in the price of asphalt cement." *J. Manage. Eng.* 33 (5): 04017026. https://doi.org/10.1061/(ASCE)ME.1943-5479.0000537.
- Ilbeigi, M., and B. Dilkina. 2018. "Statistical approach to quantifying the destructive impact of natural disasters on petroleum infrastructures." *J. Manage. Eng.* 34 (1): 04017042. https://doi.org/10.1061/(ASCE)ME .1943-5479.0000566.
- Kingma, D. P., and J. Ba. 2014. "Adam: A method for stochastic optimization." Preprint, submitted December 22, 2014. https://arxiv.org/abs/1412.6980.
- Klotzbach, P. J., K. M. Wood, C. J. Schreck III, S. G. Bowen, C. M. Patricola, and M. M. Bell. 2022. "Trends in global tropical cyclone activity: 1990–2021." *Geophys. Res. Lett.* 49 (6): e2021GL095774. https://doi.org/10.1029/2021GL095774.
- Levin, M. 2015. "How Hurricane Rita anxiety led to the worst gridlock in Houston history." Accessed September 22, 2015. https://www.chron.com/news/houston-texas/houston/article/Hurricane-Rita-anxiety-leads-to-hellish-fatal-6521994.php.
- Li, J., X. Mei, D. Prokhorov, and D. Tao. 2016. "Deep neural network for structural prediction and lane detection in traffic scene." *IEEE Trans. Neural Networks Learn. Syst.* 28 (3): 690–703. https://doi.org/10.1109/TNNLS.2016.2522428.
- Mahalanobis, P. C. 1936. "Mahalanobis distance." In Vol. 49 of Proc., National Institute of Science of India, 234–256. New Delhi, India: Indian National Science Academy.
- Montgomery, D. C. 2020. Introduction to statistical quality control. Hoboken, NJ: Wiley.
- Nair, V., and G. E. Hinton. 2010. "Rectified linear units improve restricted Boltzmann machines." In *Proc.*, 27th Int. Conf. on Machine Learning (ICML-10), 807–814. West Wareham, MA: Omni Press.
- Nouri, M., M. Reisi-Gahrooei, and M. Ilbeigi. 2022. "A method for granular traffic data imputation based on PARATUCK2." *Transp. Res. Rec.* 2676 (10): 220–230. https://doi.org/10.1177/03611981221089298.
- Parsa, A. B., H. Taghipour, S. Derrible, and A. K. Mohammadian. 2019. "Real-time accident detection: Coping with imbalanced data." Accid. Anal. Prev. 129 (Aug): 202–210. https://doi.org/10.1016/j.aap.2019.05.014.
- Pignatiello, J. J., and G. C. Runger. 1990. "Comparisons of multivariate CUSUM charts." J. Qual. Technol. 22 (3): 173–186. https://doi.org/10 .1080/00224065.1990.11979237.
- Sherstinsky, A. 2020. "Fundamentals of recurrent neural network (RNN) and long short-term memory (LSTM) network." *Physica D* 404 (Mar): 132306. https://doi.org/10.1016/j.physd.2019.132306.
- Siami, M., D. A. Khaburi, A. Abbaszadeh, and J. Rodríguez. 2016. "Robustness improvement of predictive current control using prediction

- error correction for permanent-magnet synchronous machines." *IEEE Trans. Ind. Electron.* 63 (6): 3458–3466. https://doi.org/10.1109/TIE .2016.2521734.
- Srinivasan, D., V. Sharma, and K. Toh. 2008. "Reduced multivariate polynomial-based neural network for automated traffic incident detection." *Neural Netw.* 21 (2–3): 484–492. https://doi.org/10.1016/j.neunet .2007.12.028.
- Srivastava, N., G. Hinton, A. Krizhevsky, I. Sutskever, and R. Salakhutdinov. 2014. "Dropout: A simple way to prevent neural networks from overfitting." J. Mach. Learn. Res. 15 (1): 1929–1958.
- Su, Z., Q. Liu, C. Zhao, and F. Sun. 2022. "A traffic event detection method based on random forest and permutation importance." *Mathematics* 10 (6): 873. https://doi.org/10.3390/math10060873.
- Tang, S., and H. Gao. 2005. "Traffic-incident detection-algorithm based on nonparametric regression." *IEEE Trans. Intell. Transp. Syst.* 6 (1): 38–42. https://doi.org/10.1109/TITS.2004.843112.
- Wu, Z., J. Jiao, M. Yang, Y. Liu, and Z. Wang. 2009. "An enhanced adaptive CUSUM control chart." *IIE Trans.* 41 (7): 642–653. https://doi.org/10.1080/07408170802712582.

- Xiao, J. 2019. "SVM and KNN ensemble learning for traffic incident detection." *Physica A* 517 (Mar): 29–35. https://doi.org/10.1016/j.physa.2018.10.060.
- Yao, B., P. Hu, M. Zhang, and M. Jin. 2014. "A support vector machine with the Tabu search algorithm for freeway incident detection." *Int. J. Appl. Math. Comput. Sci.* 24 (2): 397–404. https://doi.org/10.2478/amcs-2014-0030.
- Zhang, X., Y. Zheng, Z. Zhao, Y. Liu, M. Blumenstein, and J. Li. 2021. "Deep learning detection of anomalous patterns from bus trajectories for traffic insight analysis." *Knowl.-Based Syst.* 217 (Apr): 106833. https://doi.org/10.1016/j.knosys.2021.106833.
- Zhao, Y., J. Chu, H. Su, and B. Huang. 2010. "Multi-step prediction error approach for controller performance monitoring." *Control Eng. Pract.* 18 (1): 1–12. https://doi.org/10.1016/j.conengprac.2009.07.006.
- Zhu, J., K. Sun, S. Jia, Q. Li, W. Lin, X. Hou, B. Liu, and G. Qiu. 2018. "Urban traffic density estimation based on ultrahigh-resolution UAV video and deep neural network." *IEEE J. Sel. Top. Appl. Earth Obs. Remote Sens.* 11 (12): 4968–4981. https://doi.org/10.1109/JSTARS .2018.2879368.